Simulating diffusion on Si(001) 2×1 surfaces using a modified interatomic potential

Jun Wang and A. Rockett
Coordinated Science Laboratory, Materials Research Laboratory and the Department of Materials Science and Engineering, University of Illinois, 1101 West Green Street, Urbana, Illinois 61801
(Received 22 October 1990; revised manuscript received 7 February 1991)

A modified form of the Tersoff empirical interatomic potential for Si is proposed to improve simulation of adatom behaviors on Si surfaces. The modified form of the potential is consistent with local-density-approximation calculations of the surface electronic band structure of Si(001) 2×1. It is demonstrated that the addition of a screened-Morse-potential tail to the bulk Tersoff interaction behavior when tetrahedral coordination is disrupted improves the results significantly. The surface structure is calculated and shown to yield substantial differences with respect to the original potential form. In particular, anomalous abrupt variations in adatom bonding energy are eliminated and the probability of a successful deposition of the adatom on a lattice site is increased.

I. INTRODUCTION

Microelectronic-device applications require increasingly short-range changes in the properties of their constituent materials, in some cases over distances of one atomic layer. Great progress in forming such abrupt junctions has been achieved. However, further progress will require a more detailed understanding of surface atom dynamics. Of the technologically important materials, Si is by far the most widely used. Many theoretical[1–7] and experimental[8–11] studies of Si surfaces have been carried out in the past two decades. Average atomic positions on Si(001) and Si(111) have been characterized by a wide range of techniques including low-energy electron diffraction[8,9] (LEED) and scanning tunneling microscopy (STM).[10,11] The surfaces are observed to reconstruct and models for the reconstructions have been proposed including the dimer-chain-vacancy[12] and dimer–adatom–stacking-fault[13] atomic arrangements for the (001) and (111) faces, respectively.

Published results have given an excellent picture of the static Si surface. However, to understand adatom dynamics it is necessary to follow the motion of individual adatoms as they diffuse across a surface. Unfortunately, to date it has been impossible to observe the motion of single adatoms on these surfaces directly. To study adatom motions indirectly, computer simulations based on both the Monte Carlo[14] (MC) and molecular-dynamics[15] (MD) approaches have been developed to aid in interpretation of experimental data. The MC approach permits simulations of long-time scales but involves numerous assumptions about how atoms diffuse. These are frequently *ad hoc* in nature and consequently unreliable. The assumptions are most easily checked by direct simulation using the more fundamental MD approach. To make an accurate MD model of adatom behavior it is necessary to have an accurate, empirical, interatomic energy function. In general, previously reported interatomic potentials are inadequate for such diffusion modeling.

This paper examines atomic diffusion on Si(001) 2×1 and how this may be simulated using MD and empirical interatomic potentials for Si. The major problems with the application of one of the most popular bulk empirical potentials, the Tersoff potential, to surface diffusion are considered and improvements to the potential are suggested. Modifications presented in this paper are focused only on the interaction range and the two- or three-body nature of the potential. The angular stiffness of the potential will not be considered here. The modifications were tested by examining the behavior of atoms in bulk Si and of an adatom on the Si(001) 2×1 surface for which substantial experimental data are available. Preliminary results show that the modified potential yields better adatom behaviors than the original Tersoff potential without substantially modifying the relatively successful bulk response of the simulated material.

II. MODEL

In MD, atomic motions are determined by integrating Newton's equations as constrained by boundary conditions of the simulation and based on an empirical interaction potential. To develop an improved empirical potential for surface simulations we have considered a number of bulk interatomic potentials. We begin by reviewing this analysis on the basis of which the Tersoff potential was selected to be modified for surface simulation. We then present the modifications tested to date and the methods of evaluating these.

A. Interatomic potential

Current empirical interatomic potentials for covalently bonded materials can be divided into three major groups, according to their physical or mathematical bases. The first group, called valence-force potentials, are designed to fit the phonon-dispersion relations and small elastic deformation behaviors of the simulated structure.[16,17] Such potentials cannot be applied to systems which have large atomic displacements, such as occur at defects and sur-

faces. The second group[18] expands the interatomic force terms in increasingly collective interactions (binary, three-body, . . .). This approach emphasizes long-range bonding effects. However, it is difficult to determine the relative contributions of each of the many-body interactions to the total bonding force between atoms from either first-principles arguments or from measurements.

The last group of potentials is designed from the basic ideas of quantum chemistry and the observations of the mechanical behavior of solids.[19,20] A pair potential is modified by the local environment of the atom for which the bonding energies are to be determined. The modification, in the form of a three-body term, is adjusted to predict correctly the cohesive energy of different coordination-number geometries such as bcc or fcc. An example of this approach is the Tersoff potential[20] developed for Si. In this potential the tetrahedral structure is more stable than others due to the relatively strong bonding in low coordination geometries. The Tersoff potential has been shown to fit bulk elastic properties, high-pressure metastable amorphous states, some features of the surface reconstruction of Si(001), and polytypes of Si relatively well. The cohesive energies and bond lengths of these structures are also well reproduced. The Tersoff potential has also been used for Si(001) surface MD calculations.[15] To date, the Tersoff potential and its close relatives[21] are the only potentials which represent bulk Si behaviors successfully in such a large configuration space. However, the dynamic properties of the potential on Si surfaces are not yet well tested.

The Tersoff potential, like the other covalent potentials, has a short interaction range and a soft angular energy dependence which causes problems when it is applied to surfaces. Interatomic distances and bond angles are significantly distorted on the surface, especially during diffusion events. Adatoms and atoms forming the surface have lower symmetry than bulk atoms. As a result, bonding types other than sp^3 are found on Si(001) as shown by local-density-approximation (LDA) calculations.[5] The effects of these weakly bonding electron states must be reflected in the empirical interatomic potential to be used in a surface dynamic simulation of Si.

To form an improved potential for surface simulations, both the metallic and directional (covalent) contributions to bonding were taken into account explicitly. As a result, the modified interatomic potential interpolates between short-range covalent and screened long-range bonding among Si surface atoms. The Tersoff potential was chosen for the covalent bonding part, while at longer ranges a modified Morse potential was used. These potentials are described in detail in Refs. 20 and 22, respectively. The relevant features of each are reviewed briefly below.

The Tersoff potential includes attractive and repulsive components which decay exponentially with distance from the central atom. The range of the attractive part is slightly larger than that of the repulsive part yielding a net bonding force at a fixed range. The repulsive part is spherical in symmetry while the attractive constituent includes an angular dependence which seeks to maintain an angle $\theta \sim 127°$ between any two atoms bonded to a third atom. The angle-dependent term is quadratic in $\cos\theta$ with a form fit to energies of Si lattices of different coordination. An exponential screening term is included which prevents an atom (i) from influencing a second atom (j) when other atoms (k) lie nearly between atoms i and j. For large atom clusters and bulk lattices the diamond structure (tetrahedral symmetry) with a bond angle of $\sim 109°$ is most stable. Because the angular dependence is asymmetric with respect to distortions around the tetrahedral value the potential actually favors increasing the bond angle while it is relatively stiff as the bond angle decreases. The potential includes a cutoff function which reduces all interactions to zero according to

$$f_c(r_{ij}) = \begin{cases} 1, & r < R - D \\ 0.5 - 0.5 \sin[\pi/2(r-R)/D], & R - D < r < R + D \\ 0, & r > R + D \end{cases} , \tag{1}$$

where R is the center point of the cutoff process and $2D$ is the range over which the cutoff occurs, see Fig. 1. The value of R given by Tersoff is 0.285 nm which eliminates second-nearest-neighbor interactions in bulk Si and consequently reduces computation time in molecular-dynamics simulations. Unfortunately, this cutoff function introduces substantial errors for surface calculations, as discussed below.

The Morse potential is spherically symmetric consisting of exponentially decaying attractive and repulsive contributions (similar to the Tersoff potential without the three-body behaviors). This potential is relatively successful for describing intramolecular interactions in binary molecules. It is justified on the basis of the radial exponential decay of wave functions in isolated atoms. As such it seems appropriate to treat long-range bonding between Si atoms. Furthermore, the Morse potential is qualitatively identical to the radial portion of the Tersoff potential.

The potential proposed here is very similar to the Tersoff potential but is extended to longer ranges and includes an angle-dependent screening term in the repulsive as well as the attractive terms. The resulting potential is as follows. The total energy of the system is a sum over pair potentials for all pairs of atoms. Each pair potential V_{ij} is written, following Tersoff, as

$$V_{ij} = f_c(r_{ij})(A_{ij} e^{-\lambda_i r_{ij}} - BB_{ij} e^{-\lambda_2 r_{ij}}) , \tag{2}$$

where f_c is given by Eq. (1) and A_{ij} and λ_1 and B_{ij} and λ_2

are coefficients and characteristic lengths for the repulsive and attractive components of the potential, respectively. B_{ij} is given by

$$B_{ij}=[1-(\beta\zeta_{ij})^n]^{-1/2n}, \tag{3}$$

where B, n, and β are constants and

$$\zeta_{ij}=\sum_{k\ (\neq i,j)} f_c(r_{ik})g(\cos\theta_{ijk})e^{[\lambda_3(r_{ij}-r_{ik})]^3}. \tag{4}$$

The function $g(\cos\theta_{ijk})$ is

$$g(\cos\theta_{ijk})=1+\frac{c^2}{d^2}-\frac{c^2}{d^2+(h-\cos\theta_{ijk})^2} \tag{5}$$

and λ_3, c, d, and h are constants. The angle θ_{ijk} is the interior angle between atoms i, j, and k. These equations are identical to those used by Tersoff. The coefficient A_{ij} is given by

$$A_{ij}=A\times\begin{cases}1, & r<R_a-D_a\\ B_{ij}+(1-B_{ij})\{0.5-0.5\sin[\pi/2(r-R_a)/D_a]\}, & R_a-D_a<r<R_a+D_a\\ B_{ij} & r>R_a+D_a\end{cases} \tag{6}$$

and A is a constant. Equation (6) is the only change in the potential other than modifications of parameters considered here. We expect that it will be necessary to change the function $g(\cos\theta)$ to improve the simulation further.

For the proposed form of the potential the values of the constants λ_1, λ_2, λ_3, A, B, β, n, c, d, and h are identical to those given by Tersoff.[20] The cutoff range of the potential was extended such that $R=0.385$ nm and $D=0.015$ nm in Eq. (1). The interpolation of the repulsive portion of the potential to an angle-dependent screened form occurred at $R_a=0.325$ nm with a width parameter of $D_a=0.02$ nm. The amount of long-range bonding depends upon the local geometry of the central atom for which the energy or net force is to be calculated. The more tetrahedral the environment of a central atom is, the less the screened Morse interaction contributes to the binding energy. This approach is equivalent to assuming some partial dehybridization of bonding near the surface, contributing to or resulting from the reduction of tetrahedral symmetry, with a consequent increase in $3s$ σ-bonding character.

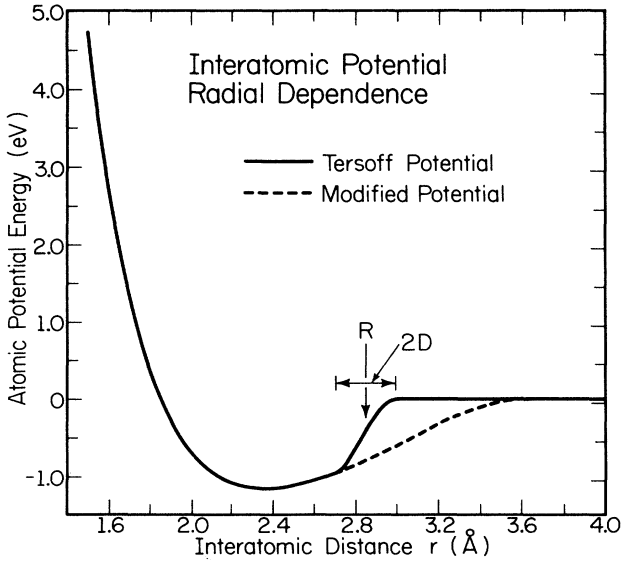

FIG. 1. Shows the radial dependence of the Tersoff potential and the modified potential. The Tersoff cutoff-region center R and width $2D$ are also shown.

B. Simulation method

In the current work the zero temperature properties of the modified Tersoff-potential solid were studied by the molecular-statics method. This locates the most stable state of the system more effectively than the quenching-dynamic method in which the surface is heated to a finite temperature, allowed to equilibrate, and quenched at some high rate to zero atomic velocity. In the molecular-statics approach, atomic motions are determined by the force acting on each of the atoms. At the end of each atomic movement any velocity gain is eliminated from the system in order to maintain zero temperature. The most stable atomic configuration is found by balancing the force on each atom, which also corresponds to the lowest potential-energy configuration. Since the force balance is determined under static conditions, care needs to be taken in choosing the starting point of the calculation in order to avoid local metastable states. The true equilibrium state was found by beginning each force minimization from a variety of relatively asymmetric starting configurations and by examining the final energy values and configurations for signs of metastability.

For the surface studies reported here, the simulation cell, consisting of one or more basis units, was slab shaped. The lower boundary condition enforced zero net motion of atoms while two-dimensional periodic boundary conditions were used around the perimeter. The basis cell in which the simplest calculations were conducted had only one column of atoms running through the slab vertically along a helix centered at the origin. A Cartesian coordinate system was used throughout the calculations with the x and y axes in the $[1\bar{1}0]$ and $[110]$ directions, respectively, and the z axis parallel to $[001]$. In each calculation the lattice was characterized by the interplanar spacing of each atomic layer in the simulation

cell and by the total energy of the system. Subtraction of the bulk energy from the energy of the solid with a surface gave the excess surface energy. The adsorption enthalpy for an adatom was calculated in a similar fashion by determining the change in total system energy for the adatom at the minimum energy position with respect to the relaxed surface without the adatom.

Minimum energy barriers for atomic motion and metastable adatom adsorption-site energies were found by mapping the surface using an adatom as a probe. To construct such maps a grid was established in the surface plane of an equilibrium reconstructed surface. An adatom was adsorbed at a point on the grid from the vapor phase with zero final velocity and the adsorption energy and position of the adatom were recorded. The adatom was always constrained to move only along the surface normal [001] during mapping. Energy topographical maps were constructed with and without concurrent relaxation of the surrounding surface atoms (see Sec. III).

The presence of an adatom on a flat surface destroys the periodicity in the surface plane locally. The embedded-dynamics technique was used when adatoms were present. Atom displacements in response to net forces were allowed only within a truncated hemispherical region (the maximum depth was less than the radius) centered on the adatom. The atoms outside the dynamic region were fixed on their initial sites. The size of the dynamic region affects the adsorption energy of the adatom which is derived in part from relaxation of the atoms in the dynamic region. The radius of the dynamic region used in this work was typically 0.8 nm. Increasing the radius beyond this value led to a fractional change in adsorption energy of less than 1%.

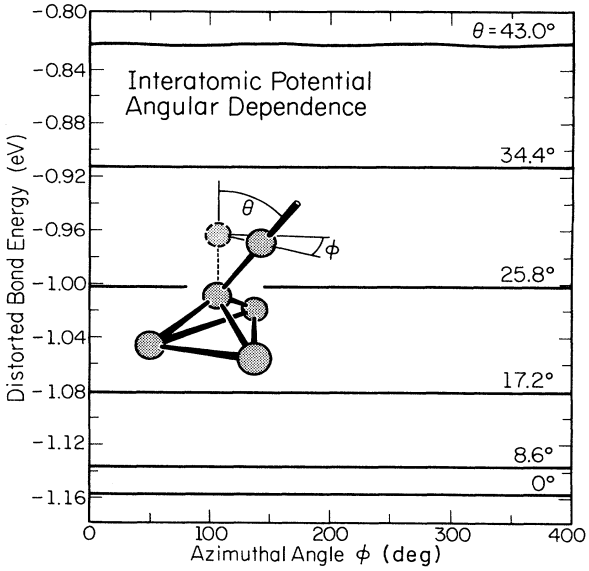

FIG. 2. The atomic potential of one atom in a five-atom body-centered tetrahedral cluster as the bond between this atom and the central atom of the cluster is distorted. The geometry of the calculation and the definition of the angles θ and ϕ are given in the inset.

III. SIMULATION RESULTS

The performance of the modified potential discussed in Sec. II A was established in four stages. The first stage was an evaluation of the behavior of the old (Tersoff) and new potentials for small atom clusters. This provided information on the radial and angular behaviors of the potentials. The second stage was a bulk-lattice simulation where three-dimensional periodic boundary conditions were used. The third stage was a flat surface calculation, in which a bulk-truncated Si(001) surface was allowed to relax to local equilibrium states with and without reconstruction. The last stage was surface mapping.

The radial component of bond energy as a function of the bond length is given in Fig. 1 for both the original Tersoff potential (solid line) and the new potential (dashed line). The interatomic force is the derivative of the energy function. Hence the abrupt cutoff of the Tersoff potential results in an attractive force well centered at 0.285 nm with a width of 0.03 nm. An atom moving away from one neighbor feels a sudden attraction when passing through the force well region. This force leads to anomalous behaviors of atoms on simulated surfaces. Such a force is not encountered for perfect bulk lattices but can be important any time the lattice is severely distorted locally. For example, large distortions occur during bulk diffusion events, ion implantation simulations, and on surfaces. The proposed modified potential eliminates the anomalous radial behavior and produces more reasonable adatom adsorption results.

The angular dependence of the original Tersoff potential was studied by distorting one bond of a five-atom body-centered tetrahedral cluster. This is essentially equivalent to studying localized motion of an adatom on a (111) surface. The distortion rotated one atom around the [111] axis while maintaining a fixed angle with respect to this axis. The result is given in Fig. 2. The distorted bond energy does not depend upon the position of the atom around the rotation circle to within 0.1%, even at relatively large distortion angles. A larger exchange interaction is expected when the rotating atom lies above the underlying atoms than that when it is between them. Si(111) surface reconstructions also show threefold symmetry[10] which would result from a periodic change in interaction strength during rotation. Adding a long-range interaction tail to the potential did not affect the results significantly. This suggests that any increase in bonding energy above an underlying atom is offset by increased distortion of the bonds through the cluster center. Hence additional changes to the angular dependence of the potential will be required if angular variations are to be produced.

Simulations were conducted to examine changes to the bulk-lattice behavior of the potential as modified. The bulk-lattice density and potential energy per atom were 49.93 atoms nm^{-3} and -4.630 eV/atom, respectively. The results show that the new potential reproduces both the structural and energetic properties of bulk Si very well as does the original Tersoff version of the potential.

TABLE I. 2×1 surface reconstruction parameters.

Value	Tersoff potential	Modified potential
Dimerization energy (eV/dimer)	−1.445	−1.614
Dimer atom spacing (nm)	0.2365	0.2360
First interlayer distance relaxation (%)	15.6	17.5

Si structures with different atomic coordinations, such as Si_2 dimer molecules, graphitic, simple cubic, bcc, and fcc, were also studied. The correct phase order for Si was obtained using the new potential with the diamond structure being the most stable. The energies of each configuration were reduced by 0.1 to 0.2 eV with respect to the Tersoff results.

A surface was produced by elimination of the top periodic boundary condition. A bulk-terminated (001) surface exhibits a large amount of surface tension, since a force balance on the surface atoms no longer exists. The interplanar distances change until interatomic repulsion balances the loss of bulk bond forces at the surface. Systems with different slab thickness were allowed to relax in order to find the depth to which atomic spacings are modified by the formation of a surface. The surface energy was found to be constant for slab thicknesses in excess of four atomic layers. Using the molecular-statics method it was possible to permit the surface to relax along (001) without reconstructing by selecting a starting configuration in which the in-plane forces were in a metastable balance. After relaxation, interplanar spacings of the slab surface were recorded as well as the excess energy per surface atom. The metastable 1×1 surface was found to have an excess energy of 2.09 eV/atom. The Si(001) 2×1 reconstruction occurred spontaneously when surface atoms were shifted slightly off their bulk positions in pairs toward each other. By alternating the direction of the shift the metastable $c(2\times2)$ reconstruction could also be generated. The dimensions and formation energy for the 2×1 reconstruction using the original and modified potentials are compared in Table I.

Table II gives the calculated atomic positions on the 2×1 reconstructed surface using the original Tersoff and the modified potentials. The reconstruction geometries predicted by the two potentials are nearly identical and agree well with calculated surface reconstructions.[5] The short-range nature of the original Tersoff potential leads to interaction of dimer atoms only with their first-nearest neighbors, namely, the other atom in the dimer pair and atoms in the second layer. With the modified potential, the positions of the third-layer atoms below the dimer row remain relatively near their lattice sites due to the weak long-range interaction with the dimer atoms. In the original Tersoff-potential case the third-layer atoms are pushed farther away from the dimer in order to optimize the bond angles. The weak interaction of the dimer and third-layer atoms found for the modified potential has been predicted by Krüger and Pollman.[5] The unpaired electron of the dimer atom dangling bond shows more *s*-like character than electrons participating directly in bonding. The open structure of the dimerized Si(001) surface leaves sufficient room for electron waves to penetrate easily beyond the second layer. These considerations support the reconstruction behavior obtained with the modified potential.

While the details of the reconstruction are of interest, they are not expected to play a major role in determining the motion of adatoms on the surface. The influence of the cutoff function of the Tersoff potential on surface diffusion has a much stronger effect, as demonstrated by the results of surface mapping studies. Surface energy topolographic maps were generated as described in Sec. II B for both the Tersoff and modified potentials. These are shown in Figs. 3 and 4. Maps constructed without surface relaxation resulting from the adatom give the structure and energy contours of the as-reconstructed surface, see Fig. 3. Diffusion energy barriers and path-

TABLE II. Atomic displacements for Si(001) 2×1 relative to the bulk-terminated surface. Definitions of axes and atom numbers are given in Fig. 5.

Atom number	Tersoff potential		Modified potential	
	Δv (nm)	Δz (nm)	Δy (nm)	Δz (nm)
11	−0.073 79	−0.019 58	−0.073 98	−0.021 29
12	0.073 79	−0.019 58	0.073 98	−0.021 29
21	−0.006 50	0.001 54	−0.002 69	0.002 48
22	0.006 50	0.001 54	0.002 68	0.002 47
31	0.000 00	0.010 93	0.000 00	0.008 92
32	0.000 00	−0.010 93	0.000 00	−0.006 91
41	0.000 00	0.006 73	0.000 00	0.005 64
42	0.000 00	−0.006 73	0.000 00	−0.005 78
51	0.003 21	0.000 00	0.002 76	0.000 00
52	−0.003 21	0.000 00	−0.002 76	0.000 00

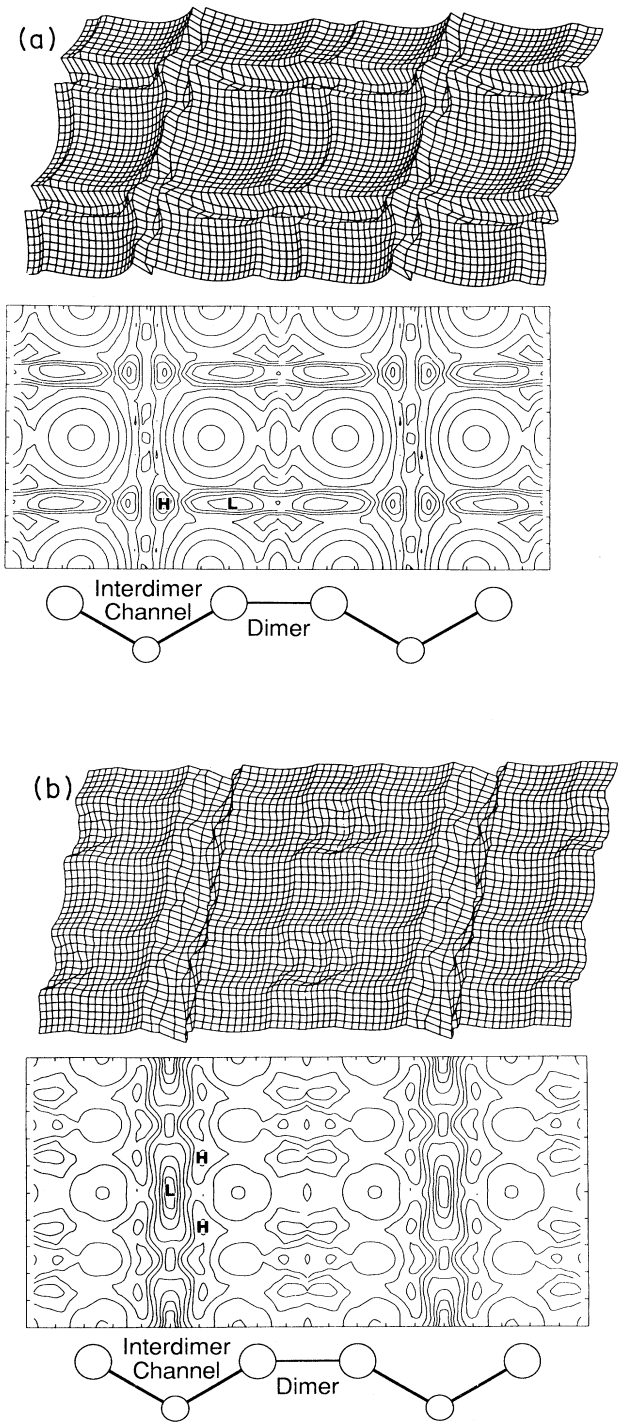

FIG. 3. Energy maps of the Si(001) 2×1 surface without relaxation. Map (a) was calculated with the unmodified Tersoff potential while (b) shows the modified potential result. Sites marked *H* and *L* are the highest (least favorable) and lowest energy, respectively. Each unit cell is symmetric and all cells are identical. Variations from symmetry result from interpolations conducted by the contour plotting program. The contour intervals are 0.18 eV for (a), 0.14 eV for (b), and the topography is shown in the isometric views.

ways which would be expected from these maps represent the fast motion limit in which the surface is unable to respond significantly to the passage of the adatom. Maps in which the surface has time to adjust completely to the presence of the adatom as it travels from one energy minimum to another represent the slow motion limit

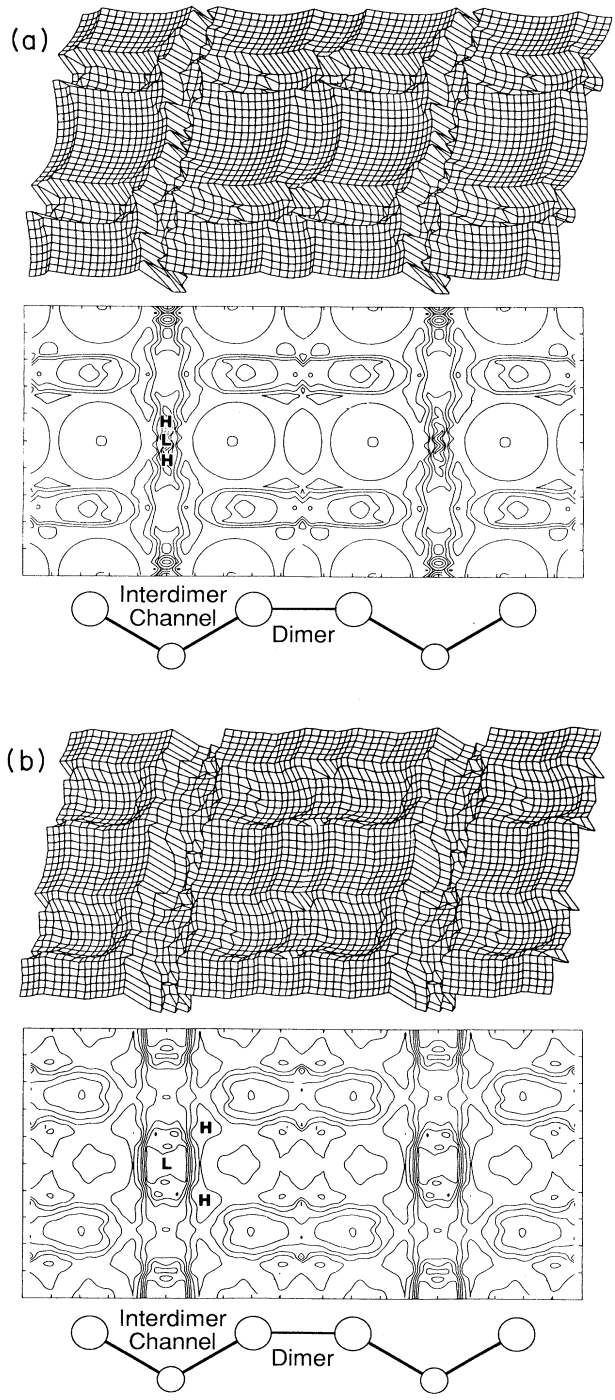

FIG. 4. Energy maps allowing the surface to relax for (a) the Tersoff potential and (b) the modified potential similar to Fig. 3. The contour intervals are 0.274 eV for (a) and 0.193 for (b).

(Fig. 4). This gives the lowest possible energy barrier to motion from one equilibrium site to another at zero temperature as well as giving the metastable adatom locations on the relaxed surface. Real adatom motion on a hot surface on which all atoms are moving would clearly differ from either of these limits. However, the general features of the maps are instructive.

IV. SURFACE DIFFUSION ON Si(001) 2×1

The results described above have significant implications for adatom diffusion and for sites on which adatoms are likely to settle after a given diffusion event is complete. While a discussion of the details of diffusion processes on Si(001) 2×1 must wait for a more complete dynamic diffusion simulation, some preliminary observations are possible. The following analysis makes use of the surface site labeling scheme illustrated in Fig. 5. Surface sites at which substantial binding can occur with the potentials considered in this paper include two lattice sites, *A* on top of the dimers and *B* in the channels between dimer rows; the dangling-bond sites *D* on the dimer atoms; and a stacking-fault site between atoms of two adjacent dimers (site *C*). For all of the calculated energy surfaces a channel between the dimer rows occurs. The features of this channel change both qualitatively and quantitatively with the type of potential and amount of allowed relaxation. On all surfaces an energy minimum occurs at the stacking-fault site, although the proposed modifications to the potential reduce the binding energy of this site significantly.

Although there are similarities, the two potentials also result in significant differences between the calculated surface maps. The Tersoff-potential surface includes prominent energy minima associated with the dangling bonds of the dimer atoms, while the modified potential produces a smoother energy "plateau" on top of the dimer row. The interdimer channel associated with the Tersoff potential lies at a higher energy than the top of the dimer row in the unrelaxed surface but below the dimer row in the fully relaxed case. The longer range of the modified potential broadens and smooths the sides of the energy minima in all cases. The modified potential places the channel well below the plateau energy for both the relaxed and unrelaxed surfaces.

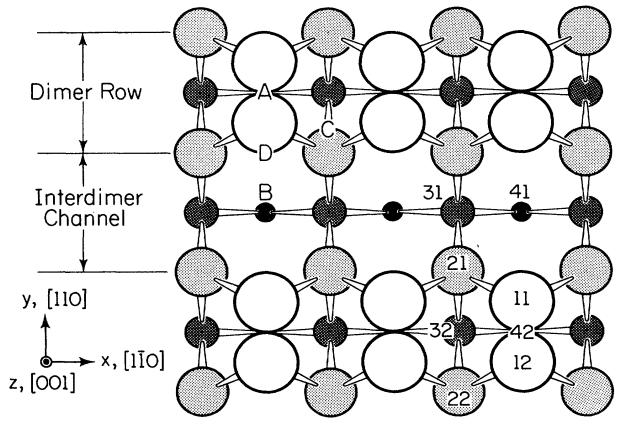

FIG. 5. A schematic top view of the Si(001) 2×1 surface labeling the sites considered in the discussion. Atoms are shaded and reduced in diameter increasingly with depth below the surface. Sites *A* and *B* are positions on the lattice in the next atomic layer. *C* is a stacking-fault site between dimer atoms. Site *D* is on the dangling bond of a single dimer atom. The numbers marking atoms on the right-hand side of the drawing refer to the atom numbers in Table II.

For both potentials the global energy minimum on the relaxed surface occurs at site *B* while site *C* provides a nearly equally favorable location. For the original potential, site *C* is stable with respect to significant changes in local atom configuration. Site *B* is unstable, relying on relaxation of the surrounding atoms to bind the adatom strongly. The modified form of the potential produces less qualitative variation in the *B* site than the *C* site upon surface relaxation. In a surface-growth simulation, this would increase the probability of epitaxial growth observed experimentally.

On the relaxed Tersoff surface, the global maximum and minimum binding energies for an adatom occur on and near lattice site *B*, respectively. As noted in Sec. III, an anomalous force develops near the cutoff range of the Tersoff potential. This force appears when an adatom is located on lattice site *B* and causes a strong attraction of the surrounding dimer atoms. This, in turn, increases the binding energy of the site. Motion of the adatom along the interdimer channel away from site *B* rapidly eliminates bonding to atoms in the adjacent dimers causing a large increase in total system energy. The resulting variations in the energy contours of the surface are nonphysical, may prevent relaxation of the lattice favoring the *B* site, and may produce unsatisfactory simulations of surface diffusion in dynamic calculations. When the potential is extended as proposed in this paper, the anomalous behavior around lattice site *B* is eliminated, the binding energy of the adatom to the relaxed surface is increased slightly at most sites, and the interdimer diffusion channel after relaxation is modified.

The static energy barriers between the major surface sites with and without surface relaxation suggest how an adatom would diffuse on the surfaces. These barriers are shown schematically in Fig. 6. Based on interpretations of experimental data,[10,11,23] it has been proposed[23] that adatoms on Si(001) 2×1 exhibit highly anisotropic diffusion. While both of the potentials mapped in Figs. 3 and 4 could yield diffusion anisotropy, significant differences between the adatom behaviors for the two potentials should exist.

The extent of anisotropy can be estimated from the energy barriers presented in Fig. 6. Although neither of the calculated limits (complete or zero relaxation) would be expected for a real adatom moving on Si(001) 2×1, the general features of the limiting cases are important. The unrelaxed surface yields adatom diffusion primarily along the tops of the dimer rows with an activation energy of 0.5–0.6 eV as the atom transfers between stacking-fault and dangling-bond sites. If the adatom could once reach the relatively high-energy interdimer channel it could

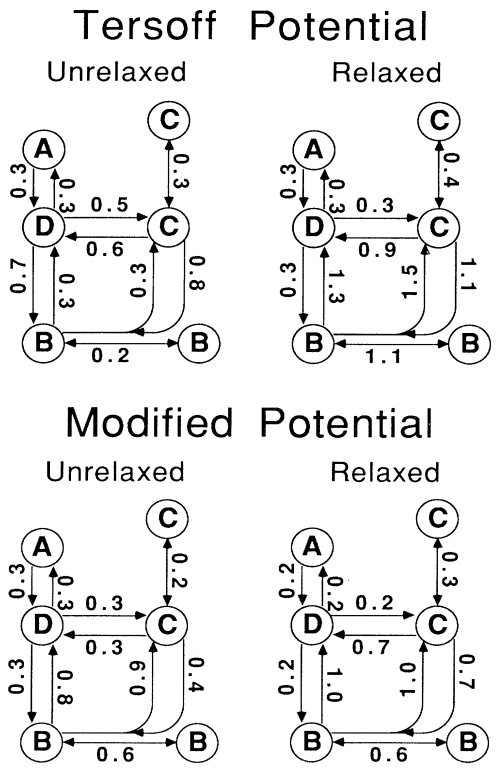

FIG. 6. A schematic diagram showing the energy barriers (in eV) to atomic motion from one site to another on the surfaces mapped in Figs. 3 and 4. The sites are labeled *A*, *B*, *C*, and *D* as defined in Fig. 5. Arrows indicate the direction of motion. Energy values which differ for opposite directions of jumps indicate the difference in energy of the end sites.

diffuse easily along the essentially uncorrugated channel bottom. Crossing the energy barrier into this channel is significantly more difficult for an adatom on the dangling bonds than to continue on to the next stacking-fault site. The difference in the two energy barriers (0.2 eV) would result in roughly a 50:1 preference at 300 °C for diffusion along the tops of the dimer rows rather than across the interdimer channel.

On the relaxed Tersoff surface the adatom would prefer to be in the interdimer channel. In this case the channel bottom is highly corrugated resulting in a diffusion activation energy of 1.1 eV. Only slightly more energy (0.2 eV) is required to transfer to the dangling-bond sites. From there it is as easy to cross the dimer row to the adjacent channel as to return to the previous channel. In summary, on the Tersoff surface a moderate preference for diffusion along the dimer rows should exist with or without surface relaxation.

The modified potential favors the adatom traveling in the interdimer channel with or without relaxation of the surface atoms. A barrier of 0.8 or 1.0 eV for the static and relaxed surfaces, respectively, prevents diffusion across the dimer rows. The activation energy along the rows is 0.6 eV. This is as much as 0.4 eV below the energy required to escape the channel, resulting in up to a 3000:1 diffusion anisotropy at 300 °C. The actual anisotropy has been estimated by Mo and Lagally[23] based on experimental results to be > 1000:1 at 300 °C. This value is more consistent with the results of the modified form of the potential than with the original form. Finally, the diffusion activation energy for the modified surface is less than that on the Tersoff surface when relaxation is allowed and comparable when relaxation is not allowed. Both potentials yield activation energies substantially larger than the experimentally determined 0.04 eV reported by Mo *et al.*[24] The value of 0.6 eV for the modified potential and for Tersoff's potential (in the absence of surface relaxation) is close to the energy calculated by Mo *et al.* based on a vibrational frequency of 10^{12} s^{-1} in the same work.[24]

The above discussion has concerned the implications of the Tersoff and modified Tersoff potentials for motion of single adatoms on Si(001) 2×1. When multiple adatoms are present significant differences may result. For example, the stacking-fault site, which is nearly as highly favored as lattice sites for a single adatom, may be less highly favored as additional adatoms accumulate. The dynamics of clusters of adatoms will be considered in a future report.

V. CONCLUSIONS

Modifications of the Tersoff empirical potential for Si should significantly improve simulation of adatom behavior on Si(001) 2×1. The modifications are consistent with interatomic interactions determined from a band-structure model of Si and Si(001) 2×1. The modified potential simulation of bulk Si is nearly identical to that of the original form. Significant reductions have been achieved in anomalous effects of the original potential resulting from its abrupt cutoff. The modified potential exhibits behaviors different from the original form for single adatoms which appear to be more consistent with the motions predicted based on experimental results.

ACKNOWLEDGMENTS

The support of the Department of Energy under Contract No. DEAC-76-ERO1198 and of IBM is gratefully acknowledged.

[1]J. A. Appelbaum, G. A. Baraff, and D. R. Hamann, Phys. Rev. Lett. **35**, 729 (1975).
[2]J. A. Appelbaum, G. A. Baraff, and D. R. Hamann, Phys. Rev. B **15**, 2408 (1977).
[3]J. A. Appelbaum and D. R. Hamann, Surf. Sci. **74**, 21 (1978).
[4]J. Ihm, M. L. Cohen, and D. J. Chadi, Phys. Rev. B **21**, 4592 (1980).
[5]P. Krüger and J. Pollman, Phys. Rev. B **38**, 10 578 (1988).
[6]B. I. Craig and P. V. Smith, Surf. Sci. **210**, 468 (1989).
[7]B. I. Craig and P. V. Smith, Surf. Sci. **218**, 569 (1989).

[8]W. S. Yang, F. Jona, and P. M. Marcus, Phys. Rev. B **28**, 2049 (1983).
[9]S. J. White, D. C. Frost, and K. A. R. Mitchell, Solid State Commun. **42**, 763 (1982).
[10]R. J. Hamers, R. M. Tromp, and J. E. Demuth, Surf. Sci. **181**, 346 (1987).
[11]R. J. Hamers, R. M. Tromp, and J. E. Demuth, Phys. Rev. B **34**, 5343 (1986).
[12]W. S. Yang, F. Jona, and P. M. Marcus, Phys. Rev. B **28**, 2049 (1983).
[13]K. Takayanagi, Y. Tanishiro, M. Takahashi, and S. Takahashi, J. Vac. Sci. Technol. A **3**, 1502 (1985).
[14]A. Rockett, Surf. Sci. **227**, 208 (1990).
[15]R. Smith, D. E. Harrison, and B. J. Garrison, Phys. Rev. B **40**, 93 (1989).
[16]Walter A. Harrison, *Electronic Structure and the Properties of Solids* (Freeman, San Francisco, 1980), Chap. 8.
[17]P. N. Keating, Phys. Rev. **145**, 637 (1966).
[18]F. Stillinger and T. Weber, Phys. Rev. B **31**, 5262 (1985).
[19]E. Pearson, T. Takai, T. Halicioglu, and W. A. Tiller, J. Cryst. Growth **70**, 33 (1984).
[20]J. Tersoff, Phys. Rev. B **38**, 9902 (1988).
[21]See Brian W. Dodson, Phys. Rev. B **35**, 2795 (1987); **36**, 1068 (1987).
[22]See Geoffrey C. Maitland, Maurice Rigby, E. Brian Smith, and William A. Wakeham, *Intermolecular Forces Their Origin and Determination* (Oxford University Press, Oxford, 1981), and references cited therein.
[23]Y.-W. Mo and M. G. Lagally, Surf. Sci. (to be published).
[24]Y.-W. Mo, R. Kariotis, B. S. Swartzentruber, M. B. Webb, and M. G. Lagally, J. Vac. Sci. Technol. A **8**, 201 (1990).